Radiotherapy and Oncology 123 (2017) 472–477

Contents lists available at ScienceDirect

Radiotherapy and Oncology

journal homepage: www.thegreenjournal.com

Prostate cancer radiotherapy

Evaluation of intensity modulated radiation therapy dose painting for localized prostate cancer using ^{68}Ga-HBED-CC PSMA-PET/CT: A planning study based on histopathology reference

Constantinos Zamboglou [a,f,*], Ilias Sachpazidis [b,f], Khodor Koubar [b,f], Vanessa Drendel [c,f], Rolf Wiehle [b,f], Simon Kirste [a,f], Michael Mix [d,f], Florian Schiller [d,f], Panayiotis Mavroidis [e], Philipp T. Meyer [d,f], Martin Werner [b,f], Anca L. Grosu [a,f], Dimos Baltas [b,f]

[a] *Department of Radiation Oncology, Medical Center – University of Freiburg, Faculty of Medicine;* [b] *Division of Medical Physics, Department of Radiation Oncology, Medical Center – University of Freiburg, Faculty of Medicine;* [c] *Department of Pathology, Medical Center – University of Freiburg, Faculty of Medicine;* [d] *Department of Nuclear Medicine, Medical Center – University of Freiburg, Faculty of Medicine, University of Freiburg, Germany;* [e] *Department of Radiation Oncology, University of North Carolina, Chapel Hill, USA; and* [f] *German Cancer Consortium (DKTK), Partner Site Freiburg, Germany*

ARTICLE INFO

Article history:
Received 1 November 2016
Received in revised form 6 April 2017
Accepted 22 April 2017
Available online 9 May 2017

Keywords:
Prostate cancer
PSMA PET/CT
Focal therapy
IMRT
Histopathology

ABSTRACT

Purpose: To demonstrate the feasibility and to evaluate the tumour control probability (TCP) and normal tissue complication probability (NTCP) of IMRT dose painting using ^{68}Ga-HBED-CC PSMA PET/CT for target delineation in prostate cancer (PCa).

Methods and materials: 10 patients had PSMA PET/CT scans prior to prostatectomy. GTV-PET was generated on the basis of an intraprostatic SUVmax of 30%. Two IMRT plans were generated for each patient: Plan^{77} which consisted of whole-prostate IMRT to 77 Gy, and Plan^{95} which consisted of whole-prostate IMRT to 77 Gy and a simultaneous integrated boost to the GTV-PET up to 95 Gy (35 fractions). The feasibility of these plans was judged by their ability to adhere to the FLAME trial protocol. TCP-histo/-PET were calculated on co-registered histology (GTV-histo) and GTV-PET, respectively. NTCPs for rectum and bladder were calculated.

Results: All plans reached prescription doses whilst adhering to dose constraints. In Plan^{77} and Plan^{95} mean doses in GTV-histo were 75.8 ± 0.3 Gy and 96.9 ± 1 Gy, respectively. Average TCP-histo values for Plan^{77} and Plan^{95} were 70% (range: 15–97%), and 96% (range: 78–100%, $p < 0.0001$). Average TCP-PET values for Plan^{77} and Plan^{95} were 55% (range: 27–82%), and 100% (range: 99–100%, $p < 0.0001$). There was no significant difference between TCP-PET and TCP-histo in Plan^{95} ($p = 0.25$). There were no significant differences in rectal ($p = 0.563$) and bladder ($p = 0.3$) NTCPs.

Conclusions: IMRT dose painting using PSMA PET/CT was technically feasible and resulted in significantly higher TCPs without higher NTCPs.

For radiotherapy (RT) of primary prostate cancer (PCa) a dose–response relationship between RT dose and tumour control rates is described. A meta-analysis postulated that the total dose of RT reduces the risk of biochemical failure by approximately 1.8% per Gy increase [1]. However, due to the proximity to rectum and bladder an unlimited dose escalation to the whole prostatic gland with external beam RT would entail an unacceptably high risk of severe toxicity [2]. Previous planning studies simulated the use of focal dose escalation on a sub-volume within the prostate, which was defined by dynamic contrast-enhanced magnetic resonance imaging (MRI), MR spectroscopy [3] or ^{11}C–choline PET/CT [4]. The latter study reported a tumour control probability (TCP) of 97% when an IMRT boost of 90 Gy was delivered to a gross tumour volume (GTV) based on 70% of SUVmax [4]. However, two more recent studies reported poor performance for choline PET/CT in PCa detection and delineation [5,6]. A multicentre, randomized trial (FLAME-trial) defined the intraprostatic boost volume by multiparametric MRI (mpMRI) [7]. The control group received 77 Gy in 35 fractions to the whole prostate. The experimental group received 77 Gy to the whole prostate with an additional integrated boost to the MRI-defined macroscopic tumour to a total dose of 95 Gy. The suspected benefit on five-year freedom from biochemical failure was at least 10% for the experimental group.

* Corresponding author at: Department of Radiation Oncology, Robert-Koch Straße 3, 79106 Freiburg, Germany.
E-mail address: constantinos.zamboglou@uniklinik-freiburg.de (C. Zamboglou).

http://dx.doi.org/10.1016/j.radonc.2017.04.021
0167-8140/

Radioactive-labelled tracers targeting the prostate specific membrane antigen (PSMA) have gained interest. PSMA is a membrane-bound enzyme and has a higher expression in malignant prostate tissue compared to benign prostate tissue [8,9]. Preliminary studies have illustrated the potential for PSMA PET/CT in the detection of primary PCa based on histology reference [10,11]. Our group compared mpMRI with PSMA PET/CT for GTV delineation in patients with primary PCa. In half of the patients discrepant results were observed [12]. Three studies compared mpMRI and PSMA PET/CT with histology after prostatectomy in patients with primary PCa. PSMA PET/CT outperformed mpMRI for PCa detection in all three studies [13–15].

Two studies compared the volumes of mpMRI and PSMA PET derived GTVs [12,16]. Both studies observed that PET based GTVs were larger than GTVs based on mpMRI. A focal dose escalation on larger GTVs implies a potential increase in toxicity for rectum and bladder.

The aim of this RT planning study was to demonstrate the technical feasibility of intensity modulated radiation therapy (IMRT) focal dose escalation on ^{68}Ga-HBED-CC PSMA PET/CT derived GTVs (GTV-PET) in patients with primary PCa. Furthermore, we calculated TCPs and the normal tissue complication probability (NTCP) for rectum and bladder.

Methods and materials

Patients

The study cohort consisted of 10 patients with intermediate (3 patients) to high-risk (7 patients) PCa [17] who had PSMA PET/CT scans prior to radical prostatectomy. In a previous study [10] a voxel-level comparison between PSMA PET and histology was performed in 9 of the 10 patients. Their characteristics are described in Supplementary Table 1. Written informed consent was obtained from each patient, and the institutional review board approved this study.

PET/CT imaging

A detailed description of our ^{68}Ga-HBED-CC-PSMA PET/CT imaging protocol can be found in Zamboglou et al. [12] for PSMA PET/CT scans using the ligand ^{68}Ga-HBED-CC-PSMA [18] were either performed with a 64-slice GEMINI TF PET/CT or a 16-slice GEMINI TF BIG BORE PET/CT (both Philips Healthcare, USA). The scanners were cross-calibrated to ensure the compatability of the quantitative measurements. Patients underwent a whole body PET scan 1 h post injection. The uptake of ^{68}Ga-PSMA-HBED-CC was quantified by standardized uptake values (SUV, regional tracer concentration normalized by injected dose per body weight).

Image co-registration

After fixation, the resected prostate underwent an ex-vivo CT scan in a customized localizer (according to our protocol [15]). Subsequently, whole-mount step sections were cut every 4 mm using an in–house cutting device and processed by an experienced pathologist (VD). The sections obtained had the same cutting angle and position as the corresponding ex-vivo CT slices. Histology sections were registered on ex-vivo CT images and PCa contours were transferred onto the CT images. The contours were expanded by 2 mm in both *Z*-axis directions to create GTV-histo. Taking into account the non-linear shrinkage and distortion of the prostatic gland after resection, ex-vivo CT (including GTV-histo) was registered on in vivo CT (from PSMA PET/CT scans) by careful manual coregistration with additional non-rigid deformation (Fig. 1). The alignment of in vivo CT and PET scan was already given by the hardware coregistration of the combined PET/CT scanners.

Generation of contours

According to our previous work [10], GTV-PET was created semi-automatically using a threshold of 30% of SUVmax within the prostate in the RT planning system iPLAN RT image 4.1 (BrainLAB, Germany). Subsequently, in vivo CT (including GTV-histo and GTV-PET) was transferred in RT planning system Oncentra v4.3 (Nucletron, The Netherlands) and contours for the prostate, seminal vesicles, and surrounding organs at risk were generated. Clinical target volume 1 (CTV1) was defined as the prostate and the seminal vesicles. CTV2 was defined as the prostate and half of the seminal vesicles (high risk patients) or the basis of the seminal vesicles (intermediate risk patients). CTV1/2 and GTV-PET were enlarged by an isotropic margin of 4 mm to create the planning target volumes (PTVs): PC1, PC2 and PC3, respectively.

IMRT planning

All CT images and contours were imported into Eclipse v13.5 (Varian, USA) and Rapid Arc IMRT treatment plans were created. The two arms of the FLAME trial [7] were simulated for each patient. The standard arm received 52.8 Gy in 24 fractions on PC1 and 24.3 Gy in 11 fractions on PC2 (Plan^{77}). The experimental arm received a concomitant boost to the PC3 with a dose of 95 Gy in 35 fractions (Plan^{95}). At least 70 Gy had to be delivered to 99% of PC2 in both arms. The D2% of PC3 had to be $\leq$105% of the prescribed dose (99.75 Gy) [19]. However, a D2% >99.75 Gy was accepted as a minor deviation.

Dose constraints for rectum and bladder were taken from the FLAME protocol [7]. Penile bulb, small bowel and sigma dose constraints were taken from the QUANTEC review [2,20,21] and have been adapted to the FLAME-trial fractionation schemes. For detailed restriction doses please see Supplementary Table 2. Adherence to the dose constraints for the organs at risk had the highest priority.

Radiobiological treatment plan evaluation

The calculations were performed in the research version of BIOTOP/BIOSPOT available in our department (provided by Pi-medical, Greece). For this purpose all DICOM RT data (images, structures, plans and doses) have been transferred from Eclipse to BIOSPOT. The summation of 3D dose distributions and EQD2 values as well as TCP and NTCP calculations were performed at the voxel level.

For Plan^{77} and Plan^{95} the differential dose-volume histogram (DDVH) for GTV-histo was generated and the corresponding average dose defined as the volume-weighted average dose ($\bar{D}$) was calculated.

For TCP modelling a radiobiological model based on the linear quadratic (LQ) Poisson model [22–29] was used (see Supplementary Material A). TCP calculations were performed for both Plan^{77} and Plan^{95} based on GTV-histo (TCP-histo) under the assumption that GTV-histo represents the true target and true clinical response, respectively.

To account for the diversity of parameters which were used for TCP calculations in current literature, we performed our TCP-histo calculation using 15 different parameter value sets (see Supplementary Material A). The following parameter ranges were used: α/β = 1.2–4 Gy, [30]; and tumour cell density $\rho = 10^5$–2.8×10^8 cells/cm^3 for intermediate and high-risk patients according to [4,31,32]. Similar to [31] for each parameter value combination the value of α was chosen in order to achieve an average TCP-histo value of 70% across all patients when Plan^{77} was used.

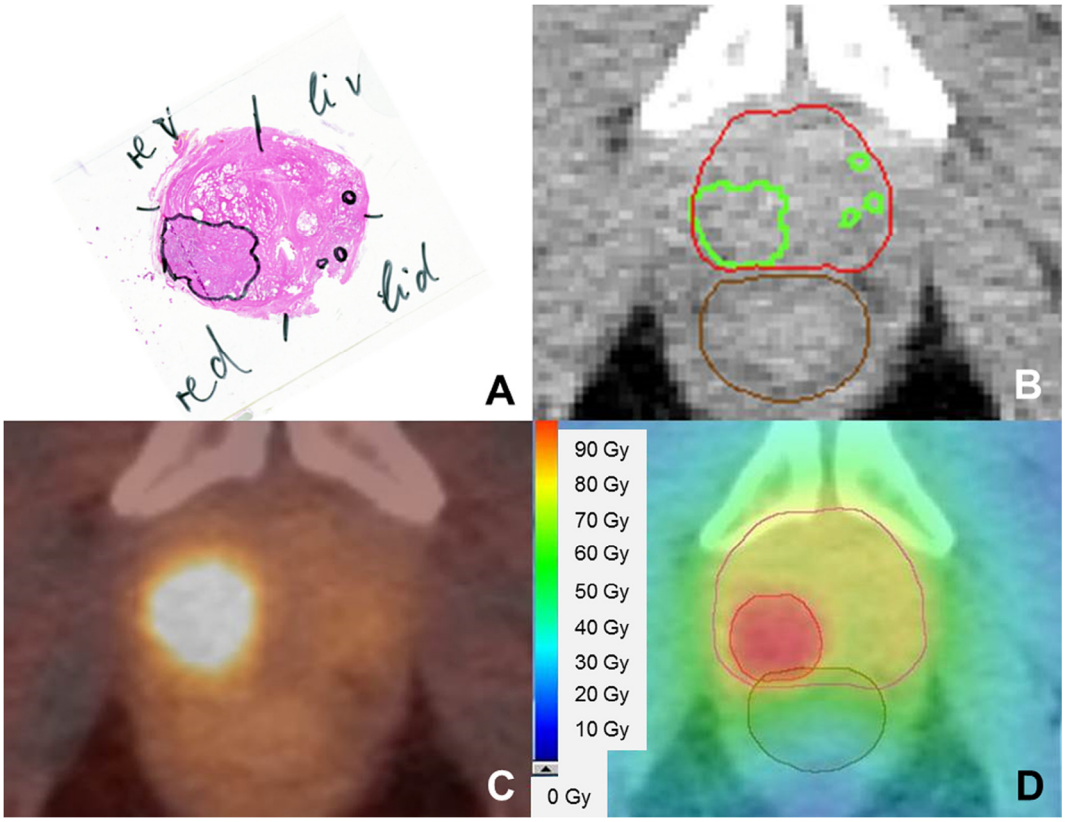

Fig. 1. Co-registration and planning procedures. (A) shows one H&E stained prostatectomy specimen of patient 1. PCa tissue was delineated with black ink. (B) shows an axial CT slice (PSMA PET/CT scan) including digitalized and registered histological information (GTV-histo, green contour). The prostate contour is marked in red. (C) shows the fused ^{68}Ga-HBED-CC-PSMA PET/CT scan, indicating PCa in the right lobe. In (D) the colourwash representation for Plan^{95} is presented. The GTV delineated with PSMA PET was expanded in all directions with a 4 mm margin to create PC3, which is marked in red.

Additionally, TCP-PET was calculated by taking GTV-PET as the tumour volume. For the calculation of TCP-PET solely parameter value set 1 was used: $\alpha/\beta = 1.93$ Gy, $\alpha = 0.1335$ Gy^{-1}, $\rho = 2.8 \times 10^8$ cells/cm^3.

To calculate NTCP from non-uniform dose distributions the relative seriality model was used [24,33–39] (see Supplementary Material B). For bladder a D50 = 80 Gy as EQD2 (symptomatic contracture and volume loss), $s = 1.3$ and $\gamma = 2.59$ were chosen in accordance to [40]. For rectum a D50 = 80 Gy as EQD2 (for severe proctitis/necrosis/stenosis/fistula, average of D50 values in [40–44]), s = 0.75 were chosen according to [40]. The γ-values ($\gamma = 2.59$ for bladder and $\gamma = 1.79$ for rectum) were calculated based on the listed k-values [36–38] (see Supplementary Material B). For both organs an α/β of 3 Gy was assumed according to a recent study [41].

Statistical analysis

Statistical analysis was performed with MATLAB (MATLAB R2014a, The MathWorks, USA) and Microsoft Excel 2010 (Microsoft, Redmond, USA). The Wilcoxon matched pairs signed-rank test was used with a threshold for statistical significance of <0.05.

Results

Mean volumes of GTV-PET and GTV-histo were 7.5 ± 4.8 ml and 5.4 ± 6.9 ml, respectively. This difference was not significant in paired comparison ($p = 0.2$). In all 10 patients, the target volume objectives as well as the OAR dose constraints were met with the exception of a minor deviation (D2% in PC3 > 99.75 Gy) in Plan^{95} in 7 patients.

For Plan^{77} and Plan^{95} the volume weighted average doses in GTV-histo were 76.8 ± 3 Gy and 96.9 ± 1 Gy, respectively. Fig. 2 shows the averaged dose volume histograms (DVHs) for the relevant volumes and Supplementary Fig. 1 shows for each patient the DVHs for Plan^{95} in GTV-histo and GTV-PET.

Average TCP-PET were 55% (range: 27–82%) for Plan^{77} and 100% (range: 99–100%) for Plan^{95}. Average TCP-histo values for all parameter value sets were 70% (range: 15–97%) and 96% (range: 78–100%) for Plan^{77} and Plan^{95}, respectively. TCP-histo and TCP-PET were significantly higher for Plan^{95} compared to Plan^{77} ($p < 0.0001$), respectively. Supplementary Tables 3 and 4 show a detailed presentation of the TCP-values. Mean NTCPs for bladder in Plan^{77} and Plan^{95} were 3 ± 1.2% and 2.9 ± 0.9%, respectively. The average NTCPs for rectum in Plan^{77} and Plan^{95} were 0.9 ± 0.4% and 1 ± 0.6%, respectively. No significant differences in rectal ($p = 0.563$) and bladder ($p = 0.3$) NTCPs were observed between the 2 plans.

Discussion

In the current study we examined the technical feasibility of PSMA PET/CT guided dose painting using the prescription doses and dose constraints of the FLAME trial (experimental and standard arm). TCP calculation was performed on PET information (GTV-PET) as well as on the registered histological information after prostatectomy (GTV-histo). The latter should demonstrate the actual tumour location and likewise should predict the true response.

Several RT planning studies demonstrated an increased therapeutic ratio when an intraprostatic boost was delivered to MRI or

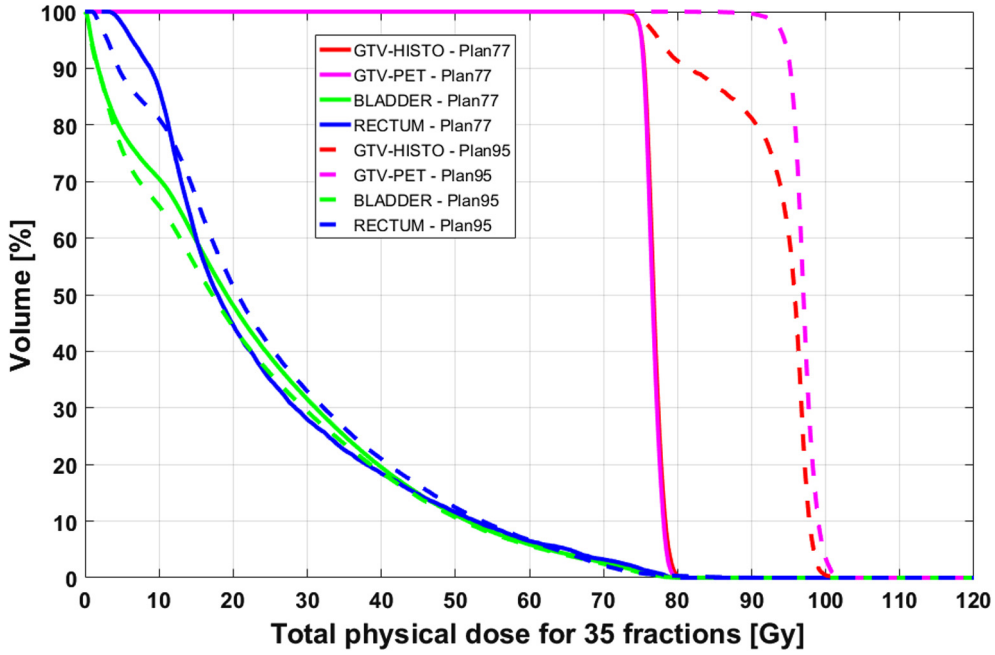

Fig. 2. Averaged DVHs. An averaged DVH, over all 10 cases, for GTV-histo, GTV-PET, bladder and rectum is shown. The dashed line represents $Plan^{95}$ and the continuous line $Plan^{77}$.

choline PET/CT based GTVs [4,41,45]. Two, multi-institutional trials included GTV boosts based on mpMRI (FLAME [7] and HEIGHT (clinicialtrials.gov NCT0141132)). Both studies delivered a GTV boost of 95 Gy with whole prostate doses in the range of 76–77 Gy. However, three studies compared mpMRI with PSMA PET/CT for detection of primary PCa based on histology Refs. [13–15] and reported higher sensitivities (49–75%) and specificities (87–95%) for PSMA PET/CT.

Our group showed that PSMA PET-based volumes (mean 11 ml) were significantly larger compared to MRI-defined volumes (mean 6 ml) [12]. This observation was also reported by Thorwarth et al. [16]. Thus, boosting of PSMA PET-defined targets may become more challenging than boosting on MRI-defined GTVs. In the present study, mean GTV-PET was larger than mean GTV-histo (7.5 ml vs. 5.4 ml), although this difference was not significant in paired analysis. This finding may be explained by the specificity of 65% when GTV-PET is delineated using a threshold of an intraprostatic SUVmax of 30% [15]. This threshold was derived from a voxel-wise correlation between PSMA PET/CT and PCa in histology using receiver operating characteristic analysis demanding a sensitivity $\geq$0.9 [10].

However, in this study the dose constraints and prescription doses of the FLAME trial [7] were applied and maintained for all patients. For $Plan^{95}$ a D2% > 99.75 Gy (EQD2 = 121.3 Gy, α/β = 1.93 Gy) in PC3 [19] was accepted as a minor deviation in 7 patients. A recent study [47], applied a cumulative dose of EQD2 = 140.9 Gy (α/β = 1.93 Gy) to GTV defined by mpMRI using 1 fraction HDR-brachytherapy in combination with hypofractionated external beam radiation therapy. With a median follow-up of 18 months none of the patients experienced acute urinary retention and only three patients (20%) experienced acute grade 2 GU toxicity. Further studies with longer follow-up are necessary to assess whether the delivery of increasing doses leads to increased genitourinary toxicity (e.g. urethral stricture). In the current study, NTCPs for bladder and rectum did not differ between dose escalation and standard RT plans using the relative seriality model. These results have been confirmed using the Lyman-Kutcher-Burman model [44] with the same α/β and D50 values. For the parameters m (slope) and n (volume) the values of 0.13 and 0.12 for bladder and 0.14 and 0.105 rectum have been used, respectively.

Niyazi et al., simulated a dose escalation based on cholin PET defined GTVs and found a dependence of different parameter values (α/β, γ50) on TCP [48]. To account for this issue, we used 15 parameter sets which included a combination of suggested values from current literature. The observed variance between the TCP-histo values for the different parameter value sets was low in our study. The average standard deviation over all datasets was 0.5% and 0.2% for $Plan^{77}$ and $Plan^{95}$, respectively.

Fig. 1 shows an exemplary case where PSMA PET failed to detect three small PCa lesions (<5 mm) in the left lobe. The lack of detection of small PCa lesions may lead to sensitivities <75% [13–15] and may be explained by PET resolution limitation [46]. In a previous study, our group performed a voxel-level correlation between PSMA PET/CT and PCa in histology [10]. A moderate correlation ($R^2 \leq 50\%$) was reported in 44% of the patients. Consequently, the present study addressed the question whether a lack in PCa detection has an influence in TCP-histo. A moderate correlation between PSMA PET/CT and PCa may explain the difference between GTV-histo and GTV-PET in the DVHs of patient 6 and 8–10 (see Supplementary Fig. 1). Despite this, we could show high TCP-histo values for $Plan^{95}$ (in mean 96%). Moreover, there was no significant difference observed when TCP was calculated on PET (TCP-PET) or histology information (TCP-histo). However, patient 9 and 10 had lower TCP-histo values compared to the other patients in $Plan^{95}$. This observation can be explained by the low coverage of GTV-histo by PSMA PET, since 76% and 88% of GTV-histo overlapped with PC3 in patient 9 and 10, respectively. On the other hand, 74% and 85% of GTV-histo overlapped with PC3 in patient 6 and 8. Both had an average TCP-histo value of 100%. The total volume of GTV-histo in patient 6 (2.7 ml), 8 (3.1 ml), 9 (40.5 ml) and 10 (31.4 ml) could explain the difference in TCP-histo values, as TCP decreases with the absolute volume of GTV-histo which is not boosted. Our findings showed the feasibility of PSMA PET/CT as a guidance tool for dose painting in primary PCa. Future studies should assess whether the additional usage of mpMRI information can lead to a further improvement of TCP, especially in patients with large tumours.

Ikeda et al. simulated the effect of intrafraction prostate motion on dose coverage of the boost volume during simultaneous boost intensity-modulated RT [49]. Since the majority of published planning studies did not investigate this effect it remains generally unknown how sensitive the coverage of GTV-histo is for dose painted PTVs to intrafractional motion. Recently, Rowe et al. defined a dominant intraprostatic lesion (DIL) as the lesion with the highest Gleason score [50]. Since data regarding the parameters to define a potential DIL are inconclusive [51,52], no separate analysis of boosting only the DIL was performed in our study. An important issue of our study is the uncertainty in the correlation of PET/CT and histopathology (e.g. manual registration between ex-vivo and in vivo CT to account for non-linear shrinkage of the prostate after prostatectomy). Thus, it could not be excluded that moderate coverage of GTV-histo by GTV-PET is partly a consequence of mismatch in coregistration or incomplete histopathological coverage instead of poor tracer performance.

Conclusion

In patients with primary PCa, IMRT dose escalation to PSMA PET/CT defined GTVs is technically feasible, achieving significantly higher TCPs based on co-registered histology without higher NTCPs compared to normal fractionation.

Funding sources

This study had no founding sources.

Conflict of interest statement

Author PTM received research grants from Piramal and GE. Author MM received research grants from Philips Medical Systems. All the other authors declare that they have no conflict of interest.

Acknowledgement

We would like to thank Colin Nolden and Mark Gainey for proof reading.

Appendix A. Supplementary data

Supplementary data associated with this article can be found, in the online version, at http://dx.doi.org/10.1016/j.radonc.2017.04.021.

References

[1] Viani GA, Stefano EJ, Afonso SL. Higher-than-conventional radiation doses in localized prostate cancer treatment: a meta-analysis of randomized controlled trials. Int J Radiat Oncol Biol Phys 2009;74:1405–18.
[2] Marks LB, Yorke ED, Jackson A, et al. Use of normal tissue complication probability models in the clinic. Int J Radiat Oncol Biol Phys 2010;76:S10–9.
[3] van Lin ENJT, Futterer JJ, Heumink SWTPJ, et al. IMRT boost dose planning on dominant intraprostatic lesions: Gold marker-based three-dimensional fusion of CT with dynamic contrast-enhanced and H-1-spectroscopic MRI. Int J Radiat Oncol Biol Phys 2006;65:291–303.
[4] Chang JH, Joon DL, Lee ST, et al. Intensity modulated radiation therapy dose painting for localized prostate cancer using C-11-choline positron emission tomography scans. Int J Radiat Oncol Biol Phys 2012;83:E691–6.
[5] Grosu AL, Weirich G, Wendl C, et al. 11C-choline PET/pathology image coregistration in primary localized prostate cancer. Eur J Nucl Med Mol Imaging 2014;41:2242–8.
[6] Bundschuh RA, Wendl CM, Weirich G, et al. Tumour volume delineation in prostate cancer assessed by [11C]choline PET/CT: validation with surgical specimens. Eur J Nucl Med Mol Imaging 2013;40:824–31.
[7] Lips IM, van der Heide UA, Haustermans K, et al. Single blind randomized phase III trial to investigate the benefit of a focal lesion ablative microboost in prostate cancer (FLAME-trial): study protocol for a randomized controlled trial. Trials 2011;12:255.
[8] Mhawech-Fauceglia P, Zhang S, Terracciano L, et al. Prostate-specific membrane antigen (PSMA) protein expression in normal and neoplastic tissues and its sensitivity and specificity in prostate adenocarcinoma: an immunohistochemical study using mutiple tumour tissue microarray technique. Histopathology 2007;50:472–83.
[9] Silver DA, Pellicer I, Fair WR, Heston WD, Cordon-Cardo C. Prostate-specific membrane antigen expression in normal and malignant human tissues. Clin Cancer Res 1997;3:81–5.
[10] Zamboglou C, Schiller F, Fechter T, et al. (68)Ga-HBED-CC-PSMA PET/CT Versus Histopathology in Primary Localized Prostate Cancer: A Voxel-Wise Comparison. Theranostics 2016;6:1619–28.
[11] Rahbar K, Weckesser M, Huss S, et al. Correlation of intraprostatic tumor extent with ^{68}Ga-PSMA distribution in patients with prostate cancer. J Nucl Med 2016;57:563–7.
[12] Zamboglou C, Wieser G, Hennies S, et al. MRI versus (68)Ga-PSMA PET/CT for gross tumour volume delineation in radiation treatment planning of primary prostate cancer. Eur J Nucl Med Mol Imaging 2016;43:889–97.
[13] Rhee H, Thomas P, Shepherd B, et al. Prostate specific membrane antigen positron emission tomography may improve the diagnostic accuracy of multiparametric magnetic resonance imaging in localized prostate cancer as confirmed by whole mount histopathology. J Urol 2016.
[14] Eiber M, Weirich G, Holzapfel K, et al. Simultaneous ^{68}Ga-PSMA HBED-CC PET/MRI improves the localization of primary prostate cancer. Eur Urol 2016.
[15] Zamboglou C, Drendel V, Jilg CA, et al. Comparison of ^{68}Ga-HBED-CC PSMA-PET/CT and multiparametric MRI for gross tumour volume detection in patients with primary prostate cancer based on slice by slice comparison with histopathology. Theranostics 2017;7:228–37.
[16] Thorwarth D, Notohamiprodjo M, Zips D, Muller AC. Personalized precision radiotherapy by integration of multi-parametric functional and biological imaging in prostate cancer: A feasibility study. Z Med Phys 2016.
[17] Mohler J, Bahnson RR, Boston B, et al. NCCN clinical practice guidelines in oncology: prostate cancer. J Natl Compr Canc Netw 2010;8:162–200.
[18] Eder M, Neels O, Muller M, et al. Novel preclinical and radiopharmaceutical aspects of [68Ga]Ga-PSMA-HBED-CC: a new PET tracer for imaging of prostate cancer. Pharmaceuticals (Basel) 2014;7:779–96.
[19] Andrzejewski P, Kuess P, Knausl B, et al. Feasibility of dominant intraprostatic lesion boosting using advanced photon-, proton- or brachytherapy. Radiother Oncol 2015;117:509–14.
[20] Fowler JF. The radiobiology of prostate cancer including new aspects of fractionated radiotherapy. Acta Oncol 2005;44:265–76.
[21] McDonald AM, Baker CB, Shekar K, et al. Reduced radiation tolerance of penile structures associated with dose-escalated hypofractionated prostate radiotherapy. Urology 2014;84:1383–7.
[22] Munro TR, Gilbert CW. The relation between tumour lethal doses and the radiosensitivity of tumour cells. Br J Radiol 1961;34:246–51.
[23] Brahme A, Agren AK. Optimal dose distribution for eradication of heterogeneous tumours. Acta Oncol 1987;26:377–85.
[24] Lind BK, Mavroidis P, Hyodynmaa S, Kappas C. Optimization of the dose level for a given treatment plan to maximize the complication-free tumor cure. Acta Oncol 1999;38:787–98.
[25] Wheldon TE, Deehan C, Wheldon EG, Barrett A. The linear-quadratic transformation of dose-volume histograms in fractionated radiotherapy. Radiother Oncol 1998;46:285–95.
[26] Yorke ED. Modeling the effects of inhomogeneous dose distributions in normal tissues. Semin Radiat Oncol 2001;11:197–209.
[27] Tucker SL, Taylor JM. Improved models of tumour cure. Int J Radiat Biol 1996;70:539–53.
[28] Zaider M, Minerbo GN. Tumour control probability: a formulation applicable to any temporal protocol of dose delivery. Phys Med Biol 2000;45:279–93.
[29] Kauweloa KI, Gutierrez AN, Bergamo A, Stathakis S, Papanikolaou N, Mavroidis P. Practical aspects and uncertainty analysis of biological effective dose (BED) regarding its three-dimensional calculation in multiphase radiotherapy treatment plans. Med Phys 2014;41.
[30] Vogelius IR, Bentzen SM. Meta-analysis of the alpha/beta ratio for prostate cancer in the presence of an overall time factor: bad news, good news, or no news? Int J Radiat Oncol Biol Phys 2013;85:89–94.
[31] Casares-Magaz O, van der Heide UA, Rorvik J, Steenbergen P, Muren LP. A tumour control probability model for radiotherapy of prostate cancer using magnetic resonance imaging-based apparent diffusion coefficient maps. Radiother Oncol 2016;119:111–6.
[32] Ghobadi G, de Jong J, Hollmann BG, et al. Histopathology-derived modeling of prostate cancer tumor control probability: implications for the dose to the tumor and the gland. Radiother Oncol 2016;119:97–103.
[33] Kallman P, Agren A, Brahme A. Tumour and normal tissue responses to fractionated non-uniform dose delivery. Int J Radiat Biol 1992;62:249–62.
[34] Lyman JT. Complication probability as assessed from dose-volume histograms. Radiat Res Suppl 1985;8:S13–9.
[35] Kutcher GJ, Burman C. Calculation of complication probability factors for non-uniform normal tissue irradiation: the effective volume method. Int J Radiat Oncol Biol Phys 1989;16:1623–30.
[36] Adamus-Gorka M, Mavroidis P, Lind BK, Brahme A. Comparison of dose response models for predicting normal tissue complications from cancer radiotherapy: application in rat spinal cord. Cancers (Basel) 2011;3:2421–43.
[37] Niemierko A, Goitein M. Calculation of normal tissue complication probability and dose-volume histogram reduction schemes for tissues with a critical element architecture. Radiother Oncol 1991;20:166–76.

[38] Schultheiss TE, Orton CG, Peck RA. Models in radiotherapy: volume effects. Med Phys 1983;10:410–5.
[39] Mavroidis P, Laurell G, Kraepelien T, Fernberg JO, Lind BK, Brahme A. Determination and clinical verification of dose-response parameters for esophageal stricture from head and neck radiotherapy. Acta Oncol 2003;42:865–81.
[40] Takam R, Bezak E, Yeoh EE, Marcu L. Assessment of normal tissue complications following prostate cancer irradiation: Comparison of radiation treatment modalities using NTCP models. Med Phys 2010;37:5126–37.
[41] Kuang Y, Wu L, Hirata E, Miyazaki K, Sato M, Kwee SA. Volumetric modulated arc therapy planning for primary prostate cancer with selective intraprostatic boost determined by 18F-choline PET/CT. Int J Radiat Oncol Biol Phys 2015;91:1017–25.
[42] Liu M, Moiseenko V, Agranovich A, et al. Normal Tissue Complication Probability (NTCP) modeling of late rectal bleeding following external beam radiotherapy for prostate cancer: a test of the QUANTEC-recommended NTCP model. Acta Oncol 2010;49:1040–4.
[43] Peeters ST, Hoogeman MS, Heemsbergen WD, Hart AA, Koper PC, Lebesque JV. Rectal bleeding, fecal incontinence, and high stool frequency after conformal radiotherapy for prostate cancer: normal tissue complication probability modeling. Int J Radiat Oncol Biol Phys 2006;66:11–9.
[44] Michalski JM, Gay H, Jackson A, Tucker SL, Deasy JO. Radiation dose-volume effects in radiation-induced rectal injury. Int J Radiat Oncol Biol Phys 2010;76:S123–129.
[45] van Lin EN, Futterer JJ, Heijmink SW, et al. IMRT boost dose planning on dominant intraprostatic lesions: gold marker-based three-dimensional fusion of CT with dynamic contrast-enhanced and 1H-spectroscopic MRI. Int J Radiat Oncol Biol Phys 2006;65:291–303.
[46] Souvatzoglou M, Weirich G, Schwarzenboeck S, et al. The sensitivity of [11C]choline PET/CT to localize prostate cancer depends on the tumor configuration. Clin Cancer Res 2011;17:3751–9.
[47] Gomez-Iturriaga A, Casquero F, Urresola A, et al. Dose escalation to dominant intraprostatic lesions with MRI-transrectal ultrasound fusion High-Dose-Rate prostate brachytherapy. Prospective phase II trial. Radiother Oncol 2016;119:91–6.
[48] Niyazi M, Bartenstein P, Belka C, Ganswindt U. Choline PET based dose-painting in prostate cancer–modelling of dose effects. Radiat Oncol 2010;5:23.
[49] Ikeda I, Mizowaki T, Ono T, et al. Effect of intrafractional prostate motion on simultaneous boost intensity-modulated radiotherapy to the prostate: a simulation study based on intrafractional motion in the prone position. Med Dosim 2015;40:325–32.
[50] Rowe SP, Gage KL, Faraj SF, et al. 18F-DCFBC PET/CT for PSMA-based detection and characterization of primary prostate cancer. J Nucl Med 2015;56:1003–10.
[51] Ravery V, Chastang C, Toublanc M, Boccon-Gibod L, Delmas V, Boccon-Gibod L. Percentage of cancer on biopsy cores accurately predicts extracapsular extension and biochemical relapse after radical prostatectomy for T1–T2 prostate cancer. Eur Urol 2000;37:449–55.
[52] Haffner MC, Mosbruger T, Esopi DM, et al. Tracking the clonal origin of lethal prostate cancer. J Clin Invest 2013;123:4918–22.